INTERPARTICLE FORCES FOR DEM BY MD SIMULATIONS

M.E.F. Apol, H.J.C. Berendsen, A.E. Mark and A.C. Hoffmann*

Dept. of Biophysical Chemistry, University of Groningen, Groningen, The Netherlands
***Dept. of Physics, University of Bergen, Bergen, Norway**

One of the ingredients in Granular Dynamics (or DEM) is a description of interparticle forces. In this paper the effect of surface roughness on Hamaker and liquid bridge interactions is investigated. Three different models are used (excluded volume, stochastic roughness and explicit asperities). In general, the latter two give similar results. Roughness decreases interactions up to several orders of magnitude for rigid surfaces. To validate the analytical results on liquid bridge interactions at low humidity, molecular dynamics simulations were also performed on model systems.

INTRODUCTION

Interparticle forces determine important physical and mechanical properties of powders, such as fluidizability and flowability, which are essential for storage, transport and handling (1). Since powders form a substantial part of the materials used in the processing industry, the industrial and economic importance of understanding these forces and the resulting bulk behavior at a fundamental level is enormous. A variety of factors influence interparticle forces: chemical composition, shape, surface roughness (asperities), elasticity, adsorbed material, humidity etc. It is often difficult in practice to determine the influence of each of these factors in isolation, and hence to develop empirical models to predict the properties of powders under specific conditions (2).

Computational methods, especially the Discrete Elements Methods or Granular Dynamics, in principle offer the possibility to perform "experiments" under controlled conditions and to vary important factors independently. One of the key ingredients of such computational methods is a model of the interparticle forces, or potential of mean force (PMF). This paper describes the modeling of two important terms of such a PMF: Hamaker and liquid bridge interactions, using both theoretical descriptions and atomistic simulations (molecular dynamics). Further details of the models can be found elsewhere (3).

One of the central analytical tools that is used throughout this paper is the so-called Derjaguin approximation, in which the total force F between two spherical particles of radius R separated by a distance D, is related to the force per unit area $f(Z)$ between two *half-spaces*, see Fig. 1a. By integrating subsequent opposing circular segments of the two *half-spaces* along the path t, one obtains (4):

$$F(D) = \pi R \int_{D}^{\infty} f(Z)\, dZ \qquad (1)$$

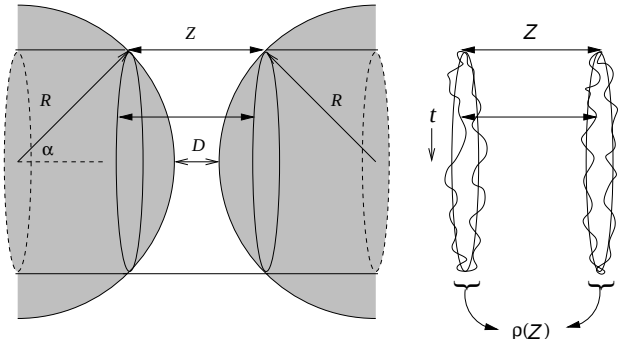

Figure 1. a. Derjaguin approximation b. Stochastic roughness model.

HAMAKER INTERACTIONS

To evaluate the Hamaker interactions due to van der Waals dispersion and Pauli repulsion, a 6-12 Lennard-Jones pair potential $u(r)=C_{12}/r^{12} - C_6/r^6$ is assumed, for which the force per unit area is

$$f_H(Z) = \rho_N^2 \pi \left[\frac{C_{12}}{45} \frac{1}{Z^9} - \frac{C_6}{6} \frac{1}{Z^3} \right] \qquad (2)$$

with ρ_N the number density. Hence, the total Hamaker force between smooth particles is

$$F_{H,s}(D) = R\, A_H \left[\frac{\sigma^6}{45} \frac{1}{8D^8} - \frac{1}{6} \frac{1}{2D^2} \right] \qquad (3)$$

using Eq. 1. $A_H = \rho_N^2 \pi^2 C_6$ is the Hamaker constant and σ the typical atomic diameter. The maximum (attractive) force $F_{H,s,max} = -R\, A_H\, (15/2)^{1/3} / 16\sigma^2$ at a distance $D_m = (2/15)^{1/6}\, \sigma$. To assess the effect of surface roughness on the Hamaker interactions, three different models will be presented.

Excluded Volume Model If particles have asperities with maximum height h_i, the minimum interparticle distance $D_{min}=2\, h_i$; hence, the effect of surface roughness could be described in the simplest way as an "excluded volume" effect. The maximum force $F_{H,r,max}$ between rough particles is approximately equal to the force between smooth particles evaluated at D_m+D_{min}: $F_{H,r,max} \cong F_{H,s}(D_m+D_{min})$. Since the leading term for large D in Eq. 3 is $O(D^{-2})$, one expects a h_i^{-2} dependence of $F_{H,r,max}/F_{H,s,max}$, as confirmed in Fig. 3 for $h_i > 1$ nm. The gravitational force is also indicated for a density of 2.65 g/cc and $A_H = 6.5 \cdot 10^{-20}$ J (4).

Stochastic Roughness Model Due to asperities, the distance z between two circular segments along the path t within the Derjaguin approximation is not constant, but fluctuates around the average value $\langle z \rangle = Z$, see Fig. 1b. Hence z can be modeled as a stochastic variable with a probability density $\rho(z)$ that reflects the surface topology. In Eq. 1, $f(Z)$ is thus corresponding to the force $f_H(z)$ given by Eq. 2, averaged over $\rho(z)$:

$$F_{H,r}(D) = \pi R \int_D^\infty \langle f_H(z) \rangle\, dZ \qquad (4)$$

Several model asperity shapes are shown in Fig. 2A-F. To each shape corresponds a specific surface height distribution $\rho(z)$: e.g. a binomial (B), the convolution of two arcsine distributions (D), or a triangular distribution (E), see Refs. (5, 6). In reality $\rho(z)$ is likely to be more or less Gaussian (7); this situation (F) is well described by a Beta(4,4) distribution (6). Fig. 3 shows that the surface morphology has a profound effect on the reduction of Hamaker

interactions for rigid surfaces. For step-like asperities resulting in a still large "average proximity" (B), the reduction is at most only a factor of 4. The average proximity decreases from semispherical (C), sine-like (D), and saw-tooth (E) to "random" asperities (F), resulting in a stronger dependency of the maximum force on the asperity height h_i: O(h_i^{-1}) for C and D, and O(h_i^{-2}) for E and F. This latter dependency is the same as for the excluded volume model. Proximity of asperities, however, increases the attractive forces with respect to the excluded volume model. Also note that already irregularities of atomic size (0.1 nm) result in a reduction of the maximum Hamaker interactions by a factor 2-3 as compared to perfectly smooth particles.

Explicit Asperities Model To validate the results of the stochastic roughness model, a third model has been developed in which the asperities are explicitly taken into account. Eq. 1 is used with $f(Z)$ the force between two flat surfaces with explicit semispherical asperities and cavities of radius h_i on a hexagonal closed-packed lattice. It is assumed that only "local" interactions between asperities and/or cavities on opposing lattice points have to be considered. These "local' interactions, in turn, are evaluated using a Derjaguin approximation. The result is shown in Fig. 3, confirming the behavior of the corresponding stochastic roughness model with semispherical asperities (C).

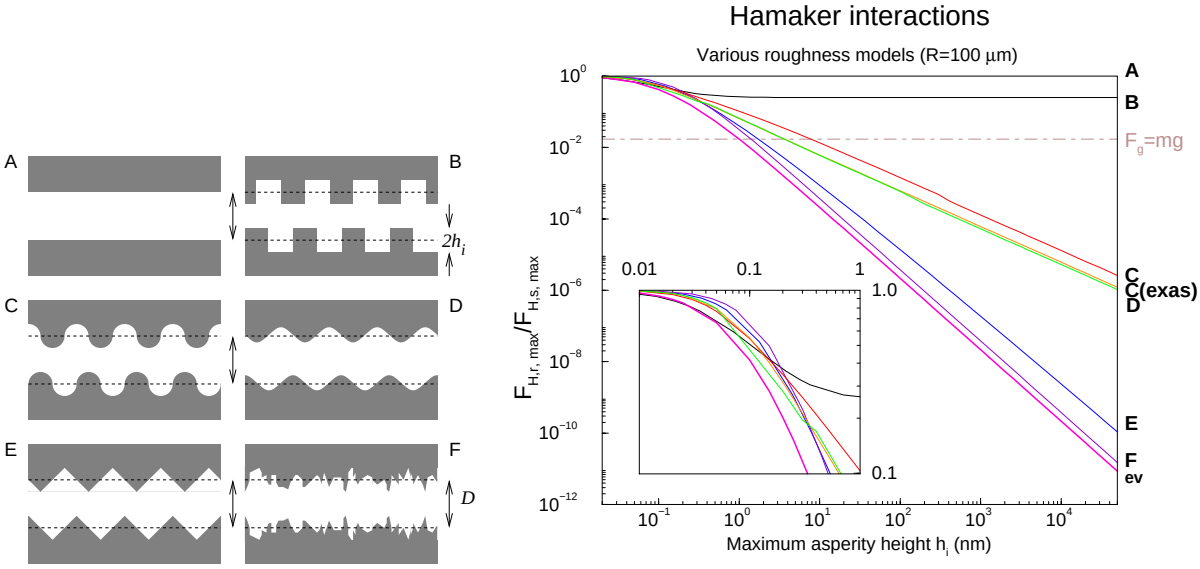

Figure 2. Various surface morphologies: A. Smooth surfaces B. Step-like asperities with maximum asperity height h_i C. Semispherical asperities D. Sine-like asperities E. Saw-tooth asperities F. "Random" asperities with Gaussian-like $\rho(z)$.

Figure 3. Ratio of the maximum Hamaker force between rough and smooth quartz particles (R=100 µm, σ=0.356 nm) for the three models: (i) Excluded volume model (ev); (ii) Stochastic roughness model for various $\rho(z)$ *corresponding to surface morphologies of Fig. 2 (A-F); (iii) Explicit asperities model (C(exas)). Gravitational forces are indicated by* F_g.

LIQUID BRIDGE INTERACTIONS

Due to capillary condensation, at relative humidities h_r below 100% water may form liquid bridges (LB) at contact points between solid bodies. The shape of these LB is determined by

the Laplace-Young equation (mechanical equilibrium), which is related to the humidity via the Kelvin equation (physico-chemical equilibrium) (8):

$$H = \frac{\mathrm{R}\,T}{2\,v_l\,\gamma}\ln(h_r) \qquad (5)$$

with H the (negative) mean curvature, R the gas constant, T the temperature, and v_l and γ the molar volume and surface tension of water. Lian *et al.* (9) have shown that a good analytical approximation to the LB shape and force is given by the "toroidal gorge" approximation, where the profile is considered to be the arc of a circle. The LB volume V_{LB} and force F_{LB} are according to (9) a function of the wetting angle θ, half filling angle φ and the half separation $S = D/2$, see Fig. 4. Usually, separation of particles is too fast to maintain physico-chemical equilibrium (10), and hence takes place at constant LB volume, so that $\varphi = \varphi_V(S)$. Lian *et al.* provide expressions for $F_{LB,s}(S;\,\theta,\,\varphi)$ and $V_{LB}(S;\,\theta,\,\varphi)$ for smooth particles. Also the mean curvature $H_{LB}(S;\,\theta,\,\varphi)$ is a function of S, θ and φ. Usually, the maximum (attractive) force occurs at close contact and is approximately $-2\pi\,R\,\gamma$. At a half separation $S_c \cong (1/2)\,(1 + \theta/2)\,V_{LB}^{\,1/3}$ the LB becomes unstable ($H_{LB}(S_c) \cong 0$) and breaks.

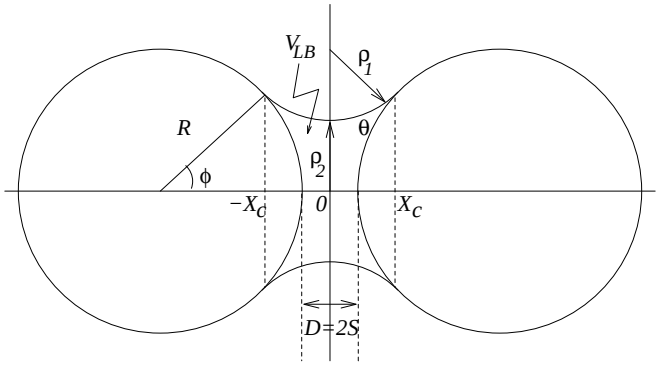

Figure 4. Geometry of a liquid bridge and definition of the quantities S, θ, and φ.

Excluded Volume Model Like for the Hamaker interactions, in this model it is assumed that particles cannot come closer than $S_{min} = h_i$. The ratio of maximum LB forces between rough and smooth particles $F_{LB,r,max}/F_{LB,s,max}$ is calculated for several values of h_i as a function of humidity, where $F_{LB,s,max} = F_{LB,s}(0;\,\theta,\,\varphi^0)$ and $F_{LB,r,max} = F_{LB,s}(h_i;\,\theta,\,\varphi^{ev})$. The angle φ^0 is evaluated from the Kelvin equation and the expression of $H_{LB}(0;\,\theta,\,\varphi^0)$, fixing θ and the humidity; the angle φ^{ev} follows from assuming that the volume $V_{LB}(h_i;\,\theta,\,\varphi^{ev})$ is equal to that of a LB between smooth particles at the same humidity, $V_{LB}(0;\,\theta,\,\varphi^0)$. (Another possibility would be to evaluate φ^{ev} from $H_{LB}(h_i;\,\theta,\,\varphi^{ev})$). Results for quartz particles at 300 K are shown in Fig. 5 with $\theta = 0°$; curves for $\theta \leq 30°$ are very similar. For comparison, the gravitational force is also indicated. Significant reduction of LB forces occurs at moderate and low humidity ($h_r < 0.9$) for asperities of at least 10 nm. At high humidity ($h_r \approx 1$), the length scale of the asperities becomes small with respect to that of the macroscopic LB; hence, the effect of roughness is minimal in that case.

Stochastic Roughness Model Although the LB force is caused by collective effects (pressure deficiency inside the LB due to curvature; surface tension), a fictitious force per unit area $f_{LB}(Z)$ can be defined via Eq. 1 as $f_{LB}(Z) = -(1/\pi\,R)(\partial F_{LB,s}/\partial Z)_{\theta,\,\varphi}$. Averaging $f_{LB}(Z)$ as for Hamaker interactions over a surface height distribution $\rho(z)$ and noting that the LB force at S_c is non-zero, one obtains in terms of the half-separation S

$$F_{LB,r}(S) = F_{LB,s}(S_c) - \int_{S}^{S_c} \left\langle \left(\frac{\partial F_{LB,s}(\zeta)}{\partial \zeta} \right)_{\theta,\varphi} \right\rangle d\zeta \qquad (6)$$

In Fig. 5 results are shown for this model using a distribution $\rho(z)$ corresponding to semispherical asperities (Fig. 2C) for h_i = 1, 10, 100 and 1000 nm. As with the Hamaker interactions, the effect of roughness predicted by the stochastic roughness model is less than that using the excluded volume model. A model with "random" asperities (Fig. 2F) will probably give results closer to the excluded volume model.

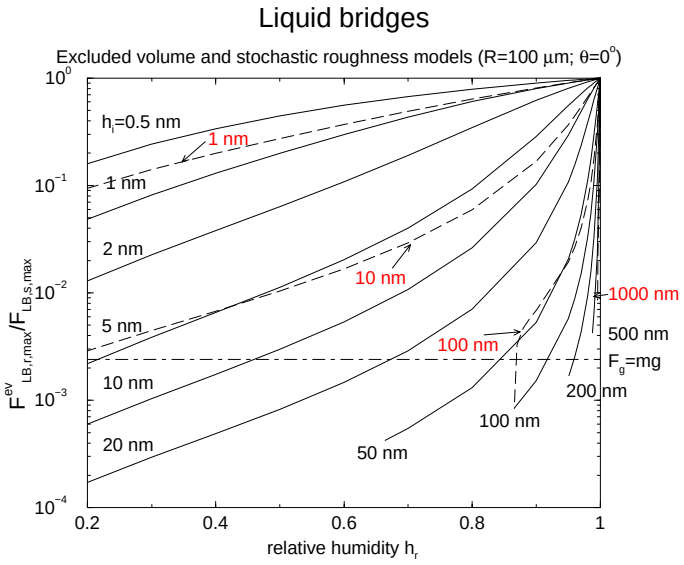

Figure 5. Ratio of the maximum liquid bridge force between rough and smooth quartz particles (R=100 μm, θ=0°): (i) Excluded volume model (solid lines) (ii) Stochastic roughness model for semispherical asperities (dashed). Gravitational forces are indicated by F_g.

Explicit Asperities Model Both previous models assume that between rough particles only a single "macroscopic" LB is being formed. However, it is likely that at lower humidity first multiple "microscopic" LB between asperities are formed. We therefore also used the same model as for the Hamaker interactions with explicit semispherical asperities and cavities of radius $h_i = h_i$[1] on a hexagonal closed-packed lattice. It is assumed that a LB may form between any pair of opposing asperities, if it is stable for that particular combination of separation and mean curvature (which, via the Kelvin equation, is given by the humidity), see Fig. 6c. The force per unit area $f_{LB}(Z)$ is calculated by summing the LB forces over all asperity-asperity couples. Note that the maximum half separation S_{max} at which the LB is still stable at a given humidity, is smaller than S_c. Since f_{LB} is very short-ranged w.r.t. the particle radius R, the total force can be evaluated via the Derjaguin approximation, Eq. 1:

$$F_{LB,r}(S) \propto \int_{S}^{S_{max}} F_{LB,s}(S', \theta, \varphi_H)\, dS' \qquad (7)$$

where $\varphi_H = \varphi_H(S)$ is evaluated from the expression $H_{LB}(S, \theta, \varphi_H)$ and the Kelvin equation. If the half filling angle φ_H is larger than the coalescense angle (30°, see Ref (11)), bridges of adjacent asperities will coalesce and the space between the particles will fill with water ("flooding", Fig. 6a, b), resulting in a "macroscopic" LB. In Fig. 7 results are presented for asperities of 10 and 1000 nm. Flooding occurs at humidity $h_{r,c}$ = 0.78 and 0.9975, respectively (points D and C), and the presence of a "macroscopic" LB dramatically

increases the attractive forces by two orders of magnitude. A further refinement of the model is to superimpose roughness of a much smaller length scale $h_i^{[2]}$ onto larger asperities (Fig. 6d). For this "second order" roughness one can follow a similar procedure as described above for "first order" roughness only. Results are shown in Fig. 7 for $h_i^{[1]}$=1000 nm asperities with $h_i^{[2]}$=10 nm roughness, reducing the interactions further by 2-3 orders as compared to 1000 nm "smooth" asperities. Note that for $h_r < h_{r,c}$, the stochastic roughness model for semispherical asperities (Fig. 5) and the explicit asperities model (Fig. 7) give for 10 nm asperities quantitatively very similar results, validating the basic assumptions of Eq. 6. However, in general the explicit asperities model should give a more accurate description.

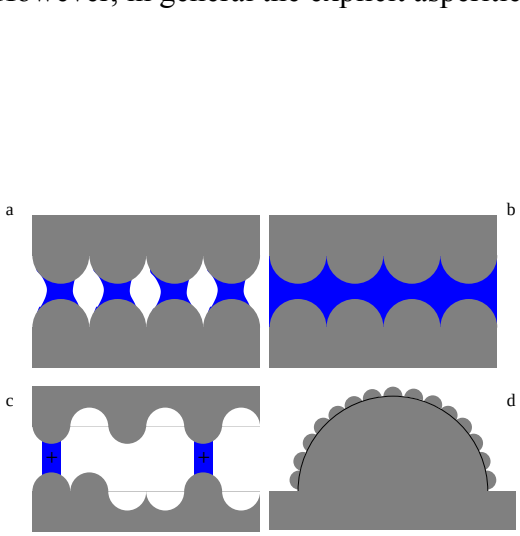

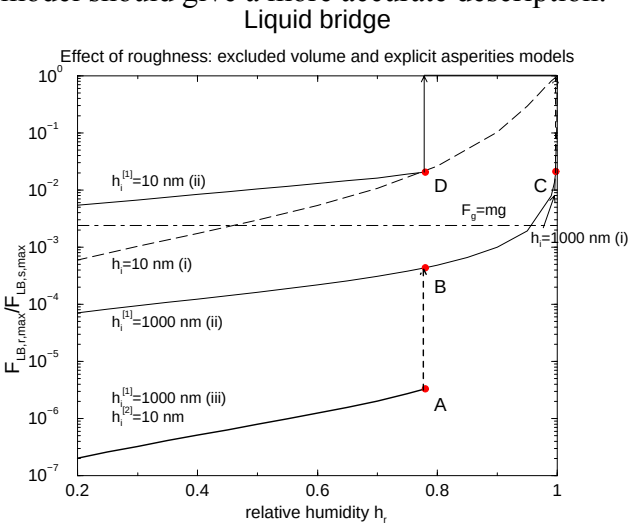

Figure 6. a, b. Coalescence of liquid bridges ("flooding") c. LB between opposing asperities on a hexagonal lattice. d. Roughness of second order.
Figure 7. Ratio of maximum LB force between rough and smooth quartz particles (cf. Fig. 5): (i) Excluded volume model (dashed lines) (ii) Explicit asperities model with roughness of first order (thin lines) and first and second order (thick lines).

MOLECULAR DYNAMICS SIMULATIONS

The expression of F_{LB} within the toroidal gorge approximation may become unreliable at low humidity where the mean curvature is of molecular dimensions (11). Moreover, in this regime the oscillatory or solvation force (4) may also become relevant. To validate the previous analytical results of liquid bridge interactions at low and intermediate humidity, molecular dynamics (MD) simulations (12) were performed to directly calculate forces due to "microscopic" LB between asperities. In a pilot study (13), simulations were performed with two opposing flat α-quartz surfaces with adsorbed water in between. For an asperity-asperity separation of 3.0 nm, a liquid bridge formed spontaneously.

With molecular dynamics, the classical equations of motion are numerically solved for a large number of particles (12). Forces are determined from the atomic positions using a potential energy function, the "force field", that includes bonded interactions (bond and angle stretching, dihedrals, constraints) and non-bonded interactions (van der Waals dispersion, Pauli repulsion, electrostatics). To avoid size artefacts, periodic boundary conditions are applied to the simulation box. The timestep for integrating the equations of motion is typically 1 fs. Since van der Waals forces are relatively short-ranged, they are evaluated with a cut-off length of typically 1.4 nm to reduce the number of interactions.

For the present simulations, starting configurations of two opposing surfaces of hexagonal closed-packed atoms were constructed with two water layers in between. The thickness of the solid layers was larger than the cut-off of the van der Waals forces (ca. 2 nm). During the simulations, these bulk surface atoms were immobile. To increase hydrophilicity of the surface, OH groups were added at a density of 4.2 nm^{-2}, mimicking quartz. These surface groups could move due to interactions with water molecules. To mimick asperities, the atoms of one or both surfaces were shifted along the z-axis (normal to the surfaces) according to the equation $\Delta z = h_i \cos(2\pi x/L_x) \cos(2\pi y/L_y)$ with L_x and L_y the x and y dimensions of the periodic box. Charges on O, H and the surface atom to which the hydroxy group was attached were taken from Ref (13). Bulk surface atoms interact via a Lennard-Jones potential mimicking quartz ($C_6 = 5.21 \cdot 10^{-3}$ kJ nm^6/mol, $C_{12} = 4.60 \cdot 10^{-6}$ kJ nm^{12}/mol). The total system with x and y dimensions of 6-8 nm typically containings 20 000-25 000 atoms. In a series of different simulations, the distance Z between the surfaces was varied (Fig. 8a), as well as the asperity dimensions (h_i, L_x and L_y), humidity (amount of water) and the hydrophilicity of the surface (interaction parameters, presence of OH-groups, surface charges). In this way, the force per unit area $f_{LB}(Z)$ could be systematically evaluated as a function of these factors by measuring the total force in the z-direction on all atoms of each surface during the simulations (13).

The Gromacs 3.0 simulation package was used (14). Long-range electrostatic interactions were treated using 3D Particle Mesh Ewald summation; to avoid artefacts since the system is quasi-2D, at the bottom and top of the simulation box a layer of vacuum was added (see Fig. 8a). Temperature was kept constant with a Berendsen thermostat (15). The SPC model was used for the water molecules (16). Snapshots of simulations with one or two curved surfaces and spontaneously formed LB are shown in Fig. 8b and c. Currently, simulations are still running to obtain enough accuracy on the measured LB forces.

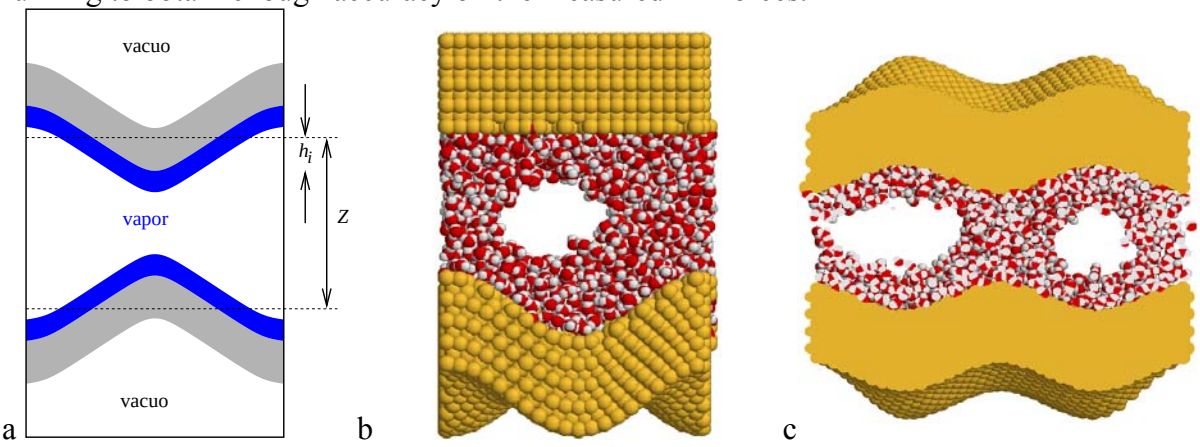

Figure 8. a. Schematic setup of simulation box b. Snapshot of a simulation with one curved surface and one liquid bridge (h_i=0.7 nm, Z=3.7 nm) c. Snapshot of a simulation with two curved surfaces and two bridges (h_i=0.7 nm, Z=3.9 nm).

CONCLUDING REMARKS

The predictions of the models as regarding the effect of surface roughness on Hamaker and liquid bridge interactions is at least qualitatively in agreement with experiments on “rigid’ particles (1) and the effect of flow conditioners. Elastic and/or plastic deformation of the surfaces will partly cancel this effect (17). Molecular dynamics simulations provide a useful

tool to investigate the effects of roughness at low humidity, where “macroscopic” theory is questionable.

MEFA acknowledges financial support from the Dutch Technology Foundation STW. The authors would especially like to thank E.J.W. Wensink, J.A.H. de Jong, S. H. Schaafsma and K. van der Voort Maarschalk for stimulating discussions.

REFERENCES

1) Seville J P K, Willett C D and Knight P C (2000) Interparticle forces in fluidization: a review. *Powder Technol. 113*, pp 261-268.
2) de Jong J A H, Hoffmann A C and Finkers H J (1999) Properly determine powder flowability to maximize plant output. *Chem. Eng. Progress 95(4)*, pp 25-33.
3) Apol M E F, Berendsen H J C, Mark A E and Hoffmann A C. Effect of surface roughness on interparticle forces of powder systems. Manuscript in preparation.
4) Israelachvili J N (1992) *Intermolecular and surface forces.* (Academic Press, London).
5) Johnson N L, Kotz S and Kemp A W (1992) *Univariate discrete distributions.* (Wiley, New York, 2nd ed).
6) Johnson N L, Kotz S and Balakrishnan N (1994, 1995) *Continuous univariate distributions (2 vols).* (Wiley, New York, 2nd ed).
7) Greenwood J A and Williamson J P B (1966) Contact of nominally flat surfaces. *Proc. R. Soc. London A 295,* pp 300-319.
8) Defay R, Prigogine I and Bellemans A (1966) *Surface tension and adsorption.* (Longmans, London).
9) Lian G, Thornton C and Adams M J (1993) A theoretical study of the liquid bridge forces between two rigid spherical bodies. *J. Colloid Interface Sci. 161*, pp 138-147.
10) Crassous J, Charlaix E, Grayvallet H and Loubet J-L (1993) Experimental study of a nanometric liquid bridge with a surface force apparatus. *Langmuir 9*, pp 1995-1998.
11) Coughlin R W, Elbirli B and Vergara-Edwards L (1982) Interparticle force conferred by capillary-condensed liquid at contact points. I. Theoretical considerations. *J. Colloid Interface Sci. 87*, pp 18-30
12) Allen M P and Tildesly D J (1987). *Computer simulation of liquids.* 385p. (Oxford University Press, Oxford).
13) Wensink E J W, Hoffmann A C, Apol M E F and Berendsen H J C (2000) Properties of adsorbed water layers and the effect of adsorbed layers on interparticle forces by liquid bridging. *Langmuir 16*, pp 7392-7400.
14) Lindahl E, Hess B and van der Spoel D (2001) Gromacs 3.0: a package for molecular simulation and trajectory analysis. *J. Mol. Model. 7*, pp 306-317.
15) Berendsen H J C, Postma J P M, van Gunsteren W F, Di Nola A and Haak J R (1984) Molecular dynamics with coupling to an external bath. *J.Chem. Phys. 81*, pp 3684-3690.
16) Berendsen H J C, Postma J P M, van Gunsteren W F and Hermans J (1981) Interaction models for water in relation to protein hydration. *In:* Pullman B (ed) *Intermolecular forces.* (Reidel, Dordrecht), pp 331-342.
17) Persson B N J and Tosatti E (2001) The effect of surface roughness on the adhesion of elastic solids. *J. Chem. Phys. 115*, pp 5597-5610.